博士論文

A recurrent *de novo FAM111A* mutation causes Kenny–Caffey syndrome type 2

(Kenny-Caffey 症候群 2 型の原因遺伝子の同定)

磯島豪

A recurrent *de novo FAM111A* mutation causes Kenny-Caffey syndrome type 2

Table of Contents

	Page
Abstract	**3**
Introduction	**4**
Subjects and Methods	**10**
Results	**19**
Discussion	**22**
Acknowledgements	**31**
References	**33**
Tables	**46**
Figures	**51**
Abbreviations	**68**

[Abstract]

Kenny–Caffey syndrome (KCS) is a very rare dysmorphologic syndrome characterized by proportionate short stature, cortical thickening and medullary stenosis of tubular bones, delayed closure of anterior fontanelle, eye abnormalities, and hypoparathyroidism. The autosomal dominant form of KCS (KCS type 2: KCS2) is distinguished from the autosomal recessive form of KCS (KCS type 1: KCS1), which is caused by mutations of the tubulin-folding cofactor E (*TBCE)* gene, by the absence of mental retardation. In this study, I recruited four unrelated Japanese patients with typical sporadic KCS2, and performed exome sequencing in three patients and their parents to elucidate the molecular basis of KCS2. The possible candidate genes were explored by a *de novo* mutation detection method. A single gene, *FAM111A* (NM_001142519.1), was shared among three families. An identical missense mutation, R569H, was heterozygously detected in all the three patients but not in the unaffected family members. This mutation was also found in an additional unrelated patient. Although the function of FAM111A is not known, this study together with the independent simultaneous report from Switzerland would provide evidence that FAM111A is a key molecule for normal bone development, height gain, and parathyroid hormone development and/or regulation.

[Introduction]

In 1966, Kenny and Linarelli first described an infant and his mother with transient hypocalcaemia, hyperphosphatemia, normal intelligence, ophthalmologic abnormalities, and severe proportionate short stature (1). Subsequently, Caffey reported the detailed radiographic findings of them (2). The distinctive findings of their roentgenogram were cortical thickening and medullary stenosis of tubular bones, and absent diploic space of the calvaria and delayed closure of the anterior fontanel. These typical radiographic characteristics of the patient analyzed in this study are shown in Figures 1 and 2. Since then, similar patients had been reported (3-7), and the constellation of these features was recognized as Kenny–Caffey syndrome (KCS).

KCS is a very rare dysmorphologic syndrome characterized by severe proportionate short stature with adult heights of 121–149 cm, cortical thickening and medullary stenosis of tubular bones, delayed closure of the anterior fontanelle, eye abnormalities, and hypocalcaemia due to hypoparathyroidism (1-4). To date, KCS has been reported in approximately 70 cases (8). Other commonly reported features in KCS are characteristic facial features (prominent forehead, micrognathia, dental anomalies, relative macrocephaly, and microcephaly), prenatal growth retardation, growth hormone deficiency, anemia, mental retardation, impaired hepatic function, microorchidism and

immunological deficiency (9-17).

Originally, KCS was thought to be transmitted in an autosomal dominant fashion (1, 2, 6, 7). In 1992, Franceschini et al. suggested that inheritance of KCS could be autosomal recessive by reporting female and male sibships with characteristic features of KCS born to normal consanguineous parents (7). In 1997, Khan showed 16 children with KCS in six unrelated families born to healthy, consanguineous parents of Kuwaiti Bedouin ancestry (18). They presented with short stature, hypoparathyroidism, radiological finding of cortical thickening of tubular bones with medullary stenosis, absent relative macrocephaly and psychomotor retardation. Through these reports it has been known that KCS is occasionally transmitted as an autosomal recessive trait. Therefore, KCS is now classified into two types according to its clinical features and inheritance pattern. Classical cases have normal intelligence and are transmitted as an autosomal dominant trait or sporadically and are called KCS type 2 (KCS2) (7). Cases having mental and prenatal growth retardation and are transmitted as an autosomal recessive trait are called KCS type 1 (KCS1) (4, 16, 19).

In Middle Eastern populations, the syndrome which had similar clinical findings to KCS1 had been reported and designated as Sanjad–Sakati syndrome (SSS) (20, 21). The cardinal features of this syndrome are congenital hypoparathyroidism,

mental retardation, facial dysmorphism, and growth failure. Thus, SSS is also known as Hypoparathyroidism–Retardation–Dysmorphism (HRD) syndrome. As SSS was a rare disorder and only found in Arab populations, it had been assumed that the disease was the result of homozygous inheritance of a recessive mutation from a common ancestor. In 1998, Parvari et al. reported that the gene for SSS was localized to 1q42–43 by homozygosity mapping for apparently unlinked kindreds (22). On the other hand, in 1998, Diaz et al. performed a genome–wide search for linkage to the gene causing KCS1 using eight consanguineous Kuwaiti Bedouin kindreds (18), and identified a significant locus at chromosome 1q42–43 (23). They also found a conserved and rare haplotype at two short tandem repeat markers (STRs) by haplotype analysis of disease–bearing chromosomes. This finding suggested that there might be a common ancestral founder mutation in the Kuwaiti KCS1 families. In addition, as the critical region for KCS1 was identical to that of SSS (1q42–43), Diaz et al genotyped eight families with SSS from Saudi Arabia with STRs from the SSS/KCS1 critical region, and demonstrated that two syndromes shared an identical haplotype (24). These studies highlighted the possibility that two syndromes were caused by the same ancestral mutation. In 2002, The HRD/ Autosomal Recessive Kenny–Caffey syndrome Consortium eventually identified mutations of the tubulin-folding cofactor E (*TBCE*)

gene as the cause of KCS1 by studying 65 individuals from 34 pedigrees of Middle Eastern origin (25). *TBCE* encodes a molecular chaperone, and it is required for heterodimerization of α-tubulin with β-tubulin (25). Intriguingly, all patients of Middle Eastern origin had a deletion of 12 base pair homozygously in the second coding exon of *TBCE*. It showed the presence of a common founder mutation in this population (25). Although clinical features of KCS2 were similar to those of KCS1, a mutation of *TBCE* had not been reported in a patient with KCS2, and the cause of KCS2 remained unknown.

For the past several decades, the gene underlying Menderian disorders had been identified through positional cloning, a process of meiotic mapping, physical mapping and candidate–gene sequencing from which the causative gene for KCS1 (i.e. *TBCE*) was elucidated (26, 27). Since 2005, next–generation DNA sequencing (NGS) technologies have become widely available and been applied for various purposes, reducing the cost of DNA sequencing by four orders of magnitude relative to Sanger sequencing (28, 29). NGS is a promising method having the potential to accelerate biological and biomedical research by enabling the comprehensive analysis of genomes. Moreover, since 2007 various technologies for capturing arbitrary subsets of a mammalian genome have been marvelously progressing at such a scale comparable to

that of massively parallel sequencing (30-34). The progress made us to perform the target sequencing of all protein–coding regions (i.e. whole–exome sequencing), which constitute less than 2% of the human genome. Figure 3 summarized the conceptual process of exome sequencing. Because most alleles that are known to underlie Menderian disorders disrupt protein–coding sequences (35), this technique is thought to be very promising for exploring causative genes for monogenic disorders (36-38). In fact, whole–exome sequencing combined with a filtering methodology was demonstrated as an approach to identify the gene underlying a Mendelian disorder using four patients' samples (27). Subsequently, it was successfully used to determine the genetic basis of both recessive and dominant Mendelian disorders with a small number of affected individuals (39-44). Moreover, by using samples of parent-child trios, *de novo* mutations were found that were responsible for rare Menderian disorders as well as for genetically heterogeneous disorders such as intellectual disabilities, schizophrenia and autism (30, 45, 46). This kind of study design is most suitable for exploring a causative gene of a disease which occurs sporadically in most cases and was suspected to be transmitted dominantly (30). Looking back on KCS2, traditional disease–gene identifications had failed to identify the causative gene for KCS2, because KCS2 is extremely rare, with only five sporadic cases reported in Japan (47-50). Thus the

identification of allelic variants for KCS2 was fundamentally limited, and the cause of KCS2 had been unknown.

In this study, I recruited four unrelated Japanese patients with typical sporadic KCS2 having normal intelligence and performed whole–exome sequencing in three unrelated parent-child trios to elucidate the molecular basis of KCS2. I hypothesized that KCS2 is caused by *de novo* mutations and built a *de novo* mutation detection pipeline to process the raw data from exome sequencing. Using this method, I found an identical *de novo* mutation in the "family with sequence similarity 111, member A" (*FAM111A*) gene (NM_001142519.1), R569H, in all four patients. While preparing for the report of my finding, another independent research group from Switzerland reported that KCS2 involved the *FAM111A* gene by following whole–exome sequencing of the patients (51). This and the reported independent studies provide the evidence that *FAM111A* is the cause of KCS2, and R569H is a hot spot mutation for KCS2.

[Subjects and Methods]

Subjects

Case 1 This 10-year-old girl (Figure 4, I-1) (47) was born at 40 weeks of gestation to non-consanguineous, healthy, Japanese parents. Polysyndactyly was noticed at birth. At three months of age, she was referred to a pediatric endocrinologist because of growth retardation. Her body length, body weight, and head circumferences were 55 cm (−2.5 SD), 5092 g (−1.8 SD), and 37.3 cm (0.2 SD), respectively. She was found to have liver dysfunction with a serum aspartate aminotransferase (AST) level of 227 U/l (reference range: 21–75) and serum alanine aminotransferase (ALT) level of 227 U/l (reference range: 11–69). Basal serum insulin-like growth factor 1(IGF-1), calcium (Ca), and phosphorus (P) levels were within normal limits. At the age of one year, hypocalcaemia was revealed. Her serum Ca, P, and intact parathyroid hormone (PTH) levels were 1.6 mmol/L (reference range: 2.1–2.4), 2.6 mmol/L (reference range: 0.88–1.4), and 11 ng/L (reference range: 15–50), respectively, with a normal magnesium (Mg) level of 0.86 mmol/L (reference range: 0.74–0.90). Her serum $1,25(OH)_2D$ level, serum alkaline phosphatase level, and urine Ca/creatinine ratio were within normal ranges. Brain computed tomography (CT) revealed calcification in the basal ganglia (Figure 5 A). She was diagnosed with primary hypoparathyroidism and was treated with

alfacalcidol [1α(OH)D_3]. At two years of age, she was diagnosed with KCS2 based on clinical manifestations of proportionate short stature, cortical thickening and medullary stenosis confirmed by radioscopic study (Figure 5 B), macrocephaly with delayed closure of the anterior fontanelle, eye abnormalities (hypermetropia and pseudopapilledema), and normal intelligence. Magnesium oxide was administered because of a low serum Mg level (below 0.62 mmol/L) at three years of age. Growth hormone therapy was initiated at nine years of age on the basis of severe growth hormone deficiency (GHD). Her height and weight at the age of 10 years 3 months were 110.8 cm (-4.2SD) and 32.5 kg (-0.2 SD), respectively.

Case 2 This 16-year-old boy (Figure 4, II-4) (48) was born at 41 weeks of gestation to non-consanguineous, healthy, Japanese parents. When he was 23 days old, he had a generalized convulsion because of hypocalcaemia. At this time, his serum Ca, P, Mg, and intact PTH levels were 1.5 mmol/L, 3.1 mmol/L, 0.74 mmol/L, and undetectable, respectively. T cell subset was normal. He was treated with alfacalcidol on the basis of a diagnosis of primary hypoparathyroidism. Magnesium sulfate was added because of his low serum Mg level at the age of one year. He suffered repeated bouts of acute otitis media until the age of two years. His serum IgG level was within the normal range. At three years and one month, his height, weight, and head circumference were 77.9 cm

(−4.4 SD), 9.9 kg (−2.7 SD), and 47.4 cm (−1.5 SD), respectively. He had normal intelligence for his age. He was diagnosed with KCS2 based on clinical findings of proportionate short stature, medullary stenosis revealed by radiography, a widely open anterior fontanelle (Figure 6 A, skull radiograph at nine years), and hypermetropia. He also suffered severe atopic dermatitis after normalization of his serum Ca levels. He had mild GHD and was treated with growth hormone, but no effect was observed. His growth chart is shown in Figure 6 B. His height at the age of 16 years was 120.6 cm (-8.2SD).

Case 3 This 22-year-old woman (Figure 4, III-9) (49) was born at 40 weeks of gestation to non-consanguineous, healthy, Japanese parents, following an uneventful pregnancy. At one month, she had an episode of generalized convulsions because of hypocalcaemia. At this episode, her serum Ca, P, Mg, and intact PTH levels were 1.3 mmol/L, 2.9 mmol/L, 0.49 mmol/L, and undetectable, respectively. Oral alfacalcidol administration was started on the basis of a diagnosis of primary hypoparathyroidism. At the age of five years one month, she was referred to another hospital. Her height was 84.2 cm (−5.3 SD), and her weight was 12.2 kg (−2.2 SD). She had normal intelligence. Brain CT revealed fine calcification in the basal ganglia. Based on clinical manifestations of proportionate short stature, medullary stenosis of the long bones

typical of KCS, a 1×1 cm opening of her anterior fontanelle, normal intelligence, and hypermetropia, she was diagnosed with KCS2. The patient was started with a combination therapy of vitamin D and magnesium sulphate. Since her short stature did not improve with this therapy, GH therapy was initiated at the age of 7 years 5 months on the basis of mild GHD, and had been continued till 17 years of age. Meanwhile gonadotropin releasing hormone analog was concomitantly administered to delay her bone maturation. Her height and weight at 22 years were 134cm (-4.5 SD) and 34kg, respectively. Figure 7 shows her radiograph at 14 years of age.

Case 4 This 38-year-old man (Figure 4, IV-13) (50) was born at 40 weeks of gestation to non-consanguineous, healthy, Japanese parents, following an uneventful pregnancy. At eight days of age, he had a generalized convulsion, and hypocalcaemia (0.75 mmol/L) and hypomagnesemia (0.18 mmol/L) were detected. The convulsion was controlled by intravenous administration of Ca gluconate and magnesium sulfate until he was 15 days old. At four years of age, he again had an episode of generalized convulsion because of hypocalcaemia. At this episode, his serum Ca, P, and intact PTH levels were 1.2 mmol/L, 2.6 mmol/L, and undetectable, respectively. He was diagnosed with primary hypoparathyroidism, and oral alfacalcidol and Ca lactate administration were started. He suffered repeated acute otitis media during infancy and was affected

with empyema and bacterial meningitis at four years of age. Hypogammaglobulinemia was found, and he was administered gamma globulin intermittently. At 12 years of age, he was referred to another hospital for further investigation. His height was 99 cm (−6.3 SD), and his weight was 16.2 kg (−3.3 SD). He had normal intelligence with an intelligence quotient score of 105. Brain CT revealed fine calcification in the basal ganglia. Based on clinical manifestations of proportionate short stature, medullary stenosis of the long bones, a 4.2 × 1.8 cm opening of his anterior fontanelle, and eye abnormalities (hypermetropia, amblyopia, and pseudopapilledema), he was diagnosed with KCS2. Mg loading and Ca restriction tests revealed that his hypoparathyroidism was secondary to hypomagnesemia. The patient was then changed from vitamin D and Ca lactate to magnesium sulfate treatment, which successfully corrected his serum Ca levels. His height at 37 years was 140cm (-5.3 SD).

I recruited these four Japanese patients with clinically diagnosed typical sporadic KCS2. Table 1 summarizes the clinical characteristics of the four patients. I obtained peripheral blood samples from all four patients, together with those of nine unaffected parents or siblings, with informed consent for DNA analysis. The study was performed with the approval of the Ethics Committee of The University of Tokyo (approved number: 2010-G3060) and of each institution where the samples were

collected, and conducted in accordance with the Declaration of Helsinki. Genomic DNA was extracted from peripheral white blood cells of the patients and family members using a QIAamp DNA Blood Midi Kit (Qiagen, Hilden, Germany). Healthy Japanese volunteers were recruited and DNA was extracted with informed consent.

Exome sequencing

Exome sequences were enriched using a TruSeq Exome Enrichment Kit (Illumina, San Diego, CA, USA) from 1 μg of genomic DNA, according to the manufacturer's instructions. The captured DNA samples were subjected to massively parallel sequencing (100 bp paired-end reads) on an Illumina HiSeq2000 sequencing system (Illumina). An average of 95 million reads of the sequence data was obtained for each individual. On an average, 98.50% of the total bases were mapped to the reference genome with a mean coverage of 140.5×, which encompassed 91.94% of the targeted regions with coverage >10× (Table 2). I built an original pipeline to process the raw data from exome sequencing under the hypothesis that KCS2 is caused by *de novo* mutations (Figure 8). The Burrows-Wheeler Aligner (BWA) package (52) and SAMtools (53) were used as default settings for alignment of raw reads and detection of single-nucleotide variants (SNVs) and indels. Subsequently, SNVs and indels were

filtered with three trio samples (i.e., pedigrees I, II, and III) (Figures 4). I extracted both homo/heterozygous non-synonymous coding variants, which were called in the proband, and filtered these candidates using the following three steps:

Step 1: Using candidate *de novo* mutations that are homozygous references in both parents and are supported by 10 or more high quality reads at the mutated sites for every trio member.

Step 2: Using reliable homozygous references in each parent such that the likelihood of heterozygosis, ${}_nC_i\,(1/2)^i\,(1/2)^{n-i}$, is less than that of homozygosis, ${}_nC_i\,(999/1000)^i(1/1000)^{n-i}$, where the average error rate is assumed to be 1/1000, n represents the number of total reads, and i is the number of reads consistent with the reference. One may have an impression that this condition does not often hold true; however, I often observed cases that violated this condition, especially when the reference base was mutated into one of the other three bases with an almost equal probability.

Step 3: Using reliable *de novo* mutations of the proband such that the number of alternative allele reads was at least 30% among the total reads, which is the condition proposed in a recent report (54).

Sanger sequencing

Sanger sequencing was performed to detect *TBCE* (KCS1) and validate the presence of each variant detected by exome sequencing in patients with KCS2 and the absence of each in the genomes of the parents and siblings. The entire coding region and exon-intron boundaries of *TBCE* and *FAM111A* were amplified from genomic DNA by polymerase chain reaction (PCR) using the designed PCR primers (Tables 3 and 4, respectively). Subsequently, sequencing was performed with PCR products using an ABI Prism BigDye Terminator Cycle Sequencing Ready Reaction Kit (PE Applied Biosystems, Foster City, CA, USA) and the forward and reverse primers used for PCR amplification. Direct sequencing in both directions was performed on an autosequencer (PE Applied Biosystems 3130×1, Genetic Analyzer).

***FAM111A* mRNA expression analysis**

Total RNA was prepared using ISOGEN reagent (Nippon Gene, Osaka, Japan), according to the manufacturer's instructions, from peripheral white blood cells of the patients and family members. Total RNA (4 μg) was used to synthesize cDNA with the SuperScript Preamplification System for first strand cDNA synthesis (Life Technologies, Rockville, MD, USA). mRNA levels were measured using an ECO real-time PCR

system (Illumina) and KAPA SYBR Fast qPCR Kit (Kapa Biosystems, Woburn, MA, USA) using the following primer pairs: FAM111Ae5-2F and FAM111Ae5-2R; FAM111Ae5-3F and 5′-CCTCATCACTCATCATTTCTACATCC-3′; GAPDH, 5′-GAAGGTGAAGGTCGGAGTC-3′ (F) and 5′- GAAGATGGTGATGGGATTTC-3′ (R). The cycle conditions were 95 °C for 1 min followed by 45 cycles of 95 °C for 5 s, 60 °C for 30 s. After completion of the reaction cycles, melting curves were obtained by heating the samples from 55 °C to 95 °C. The specificity of the primers was confirmed by the presence of a single peak in the melt curve generated for each gene. The relative mRNA level was calculated using an arithmetic formula based on the difference between the threshold cycle of a given target cDNA and that of an endogenous reference cDNA. Direct sequencing of the reverse-transcribed PCR (RT-PCR) products was performed by Sanger sequencing as for DNA samples.

[Results]

I first confirmed by Sanger sequencing that none of the four patients had *TBCE* mutations. This finding, together with the fact that all the patients were of normal intelligence, distinguishes these patients from patients with KCS1.

I hypothesized that these sporadic cases may be caused by *de novo* mutations in novel nonsynonymous coding variants. Whole exome sequencing was performed for three patients (I-1, II-4, and III-9, Figure 4) and their parents (I-2, I-3, II-5, II-6, III-10, and III-11, Figure 4). Statistical data of exome sequencing experiments are shown in Table 2. The candidate variants were selected according to the processes described in the Methods section based on the *de novo* mutation detection pipeline designed in the present study (Figure 8). Table 5 summarizes the results of filtering to detect candidate genes for KCS2. To select variants as candidate mutations for KCS2, variations that caused amino acid substitution were extracted, which resulted in 11,024 (pedigree I), 10,828 (pedigree II), and 11,020 (pedigree III) SNVs and indels. After three filtering steps, five (pedigree I), five (pedigree II), and six (pedigree III) SNVs were identified. Among the candidate genes filtered using the three aforementioned filtering steps, only one single gene, *FAM111A* (NM_001142519.1), was shared among all three families (Figure 9). Sanger sequence analysis of all exons of *FAM111A* confirmed an identical

c.1706G>A heterozygous mutation in exon 5 in all three patients (Figures 10). This mutation is predicted to result in substitution of arginine to histidine in codon 569 (R569H). None of the unaffected family members had this mutation, indicating that R569H was a *de novo* mutation. This mutation was also found in an additional unrelated patient (IV-13, Figure 10).

R569H is not present in 373 Japanese healthy control subjects of inhouse exome database, and not in another 100 alleles from 50 unrelated healthy Japanese individuals by Sanger sequencing. It was also not found in the Japanese single-nucleotide polymorphism (SNP) control database established by the National Bioscience Data Base Center that has one million genome–wide SNPs of 700 samples (http://gwas.biosciencedbc.jp/snpdb/snp_top.php), nor among 6500 samples listed on the exome variant server (http://evs.gs.washington.edu/EVS/), implying that the minor allele frequency is less than 0.01% in these data. However, one SNP was found in the 1000 Genomes database at R569 (rs184251651), which results in substitution to “cysteine” (minor allele frequency 0.1%).

I assessed the functionality of the R569H mutation using the Sorting Intolerant From Tolerant (SIFT) (http://sift.jcvi.org) and Polymorphism Phenotyping 2

(PolyPhen2) (http://genetics.bwh.harvard.edu/pph2) tools, by homology modeling and threading. These *in silico* studies predicted R569H as "tolerated" and "benign," respectively (Figure 11).

I analyzed the expression levels of *FAM111A* mRNA in peripheral white blood cells by real-time PCR. *FAM111A* expression levels in the patients were comparable with those in unaffected family members and normal controls (Figure 12). I also found that mutant and wild-type *FAM111A* were equivalently expressed in the patients, which were identified by sequencing the RT-PCR products (Figure 13).

[Discussion]

In the present study, I identified *FAM111A* as the gene responsible for KCS2 by applying an exome sequencing strategy, and I identified a heterozygous identical *de novo FAM111A* mutation, R569H, in four Japanese patients with KCS2. While preparing for this manuscript, another independent research group from Switzerland reported similar findings following whole exome sequencing of the patients with KCS2 or gracile bone dysplasia under the hypothesis that these two syndromes might be allelic disorders of different severity (51). They found that all five clinically diagnosed KCS2 patients and all five clinically diagnosed gracile bone dysplasia patients had *de novo FAM111A* mutations by using different strategy for detecting de novo mutations. Most interestingly, four of the five patients with KCS2 from different countries had the same R569H mutation as detected in the patients analyzed in this study (Figure 14). Four pedigrees investigated in the present study are unrelated to each other and live in different areas in Japan. Moreover, the parents of the three patients did not have the mutation, suggesting that this recurrent mutation was caused by sporadic mutation. As these two independent and simultaneous studies were performed with different filtering methodologies for detecting de novo mutations causative for KCS2, these studies confirm that *FAM111A* is the causative gene for KCS2, and R569H is the hot spot

mutation of KCS2, although both studies had not analyzed the function of FAM111A.

FAM111A encodes a protein consisting of 611 amino acids, and there is homology to trypsin-like peptidases in its carboxy-terminal half (Figure 14). The catalytic triad specific to such peptidases is conserved (55). At present, the function of the protein is largely unknown. According to the human protein atlas (http://www.proteinatlas.org/ENSG00000166801/normal), transcriptional expression of *FAM111A* is ubiquitous. It is expressed in the parathyroid gland and bone, but the expression levels are similar to those in other tissues. FAM111A has 35% amino acid homology to FAM111B, a paralog located on 11q12.1 at a distance of only 16 kb from FAM111A. The functions of FAM111A and FAM111B are largely unknown. Recently, FAM111A have been reported that it functions as a host range restriction factor and is required for viral replication and gene expression by interacting with Simian Virus 40 large T (LT) antigen (55). In addition, they reported that *FAM111A* mRNA and protein levels were regulated in a cell cycle-dependent manner with the lowest expression during the G0 or quiescent phase and peak expression during the G2/M phase (55). Another recent report revealed that variants in the region including *FAM111A* and *FAM111B* were associated with prostate cancer (56). However, the clinical course of disease in the four patients investigated in this study revealed neither increased viral

infections nor carcinogenesis up to early adulthood.

In silico analyses suggested that the *de novo* mutation (R569H) would not significantly affect the function of FAM111A (Figure 11). I also found that the mutant *FAM111A* mRNA was expressed similarly to the wild-type in peripheral blood cells (Figure 12). This raises the question of how this mutation causes KCS2. I hypothesize that this mutation does not cause loss of function of the protein but rather modulates its peptidase activity for a particular target peptide in a mutant-specific way. Another possibility is that FAM111A functions with some physiological partner(s) and the disease occurs as a result of specific modulation of this putative network. This may fit the observation that FAM111A is regulated in a cell-dependent manner and interacts with the LT C-terminal region (55). I speculate that one of the candidate partner proteins is TBCE because KCS1 and KCS2 share distinctive phenotypic features: skeletal dysmorphic features and primary hypoparathyroidism.

Some diseases are caused by specific mutations of a single gene. Some mutations may cause a gain-of-function effect, as in achondroplasia or McCune–Albright syndrome (57, 58), while others have an unknown function, as in Caffey syndrome caused by mutations in collagen type1 alpha 1 (*COL1A1*) gene (59) or in several diseases related to fibroblast growth factor receptor 3 (*FGFR3*) gene. In this

study, I found that a specific mutation (R569H) of *FAM111A* would lead to KCS2. Intriguingly, one SNP was found in the 1000 Genomes database at R569 (rs184251651), which results in substitution to “cysteine.” This SNP has been reported to have minor allele frequency of 0.1% (only one allele) and is not validated. Moreover, the absence of the SNP in 6500 samples in the exome variant server suggests a possibility of sequencing error in the database. Nevertheless, it might be speculated that a specific change to “histidine” may lead to an unidentified function of this protein resulting in KCS2, which is not caused by other amino acids. This hypothesis will be supported by the fact that this amino acid is not well conserved among various species (Figure 15).

It is reported that 95% and 97% of KCS1 cases had prenatal and postnatal growth retardation, and mental retardation, respectively (10). In contrast, most of the reported KCS2 patients, including our patients with *FAM111A* mutations, had normal birth weight and length, and normal intelligence (Table 1) (51). These phenotypic differences between KCS1 and KCS2 suggest that the *FAM111A* mutation does not affect bone development and height gain in the fetus but become important postnatally. It also suggests that the *FAM111A* mutation does not affect mental development. Now that *FAM111A* has been identified as a causative gene for KCS2, further studies on the physiological function of FAM111A and TBCE should be performed to uncover the

phenotypic differences between these two types (Figure 16).

There are several human diseases, as well as mouse models of hypoparathyroidism, caused by aberrations in the cascade of genes indispensable for the development and regulation of the parathyroid gland (60, 61). To date, FAM111A is not known to relate to any of these genes. There have been only a few reports describing the pathophysiology of hypoparathyroidism in KCS. Absence of the parathyroid glands has been reported in some patients with KCS2 and KCS1 (62, 63). In contrast, some patients do not have hypoparathyroidism from early infancy, suggesting the presence of some parathyroid gland as in the patient I-1 (4, 17). Furthermore, hypoparathyroidism may be secondary to hypomagnesemia as in the patient IV-13. Considering the fact that all of four patients investigated in the present study as well as another reported KCS2 case had hypomagnesemia (4), FAM111A might be involved in magnesium homeostasis. Although further investigation is necessary to reveal the cause of hypoparathyroidism in KCS2, this study shows that a new gene, *FAM111A*, is indispensable for PTH development and/or regulation.

KCS is a very rare syndrome that has been reported only in approximately 70 patients in the literatures (8), although KCS2 is an autosomal dominant disease with normal intelligence. On the other hand, achondroplasia occurs in between one in 10,000

and one in 30,000 livebirths, in which more than 95% of patients have the same mutation in *FGFR3*, G380R, and more than 80% of these patients are sporadic (64). As compared to the occurrence rate of achondroplasia, the rarity of KCS is outstanding. One possible explanation for this rarity is that patients with KCS may have gonadal hypofunction. To date, inheritance from a father-to-child has not been described regardless of an equal sex ratio of affected individuals reported in the literatures (9, 65), while the first reports of KCS was two patients which was thought to be mother-to-child transmission (1). In addition, reported pubertal or adult-age male patients with KCS had findings suggestive of microchidism or infertility (5, 6, 11, 17, 62). However, the pathogenesis of the microchidism seen in male patients with KCS remains unknown. There is only one report about this matter that hormonal investigations of male patients with KCS and microchidism showed normal sex hormones except for elevations of the follicle-stimulating hormone, and the histology of testes revealed Leydig cell hyperplasia but otherwise normal anatomy (11). It should be noted that micropenis was reported in four fifth *FAM111A* mutation positive males of the same allelic condition with KCS2, gracile bone dysplasia, by the Switzerland group (51). Although further studies will be necessary to establish the pathogenesis of male gonadal hypofunction, FAM111A may be important in the development and function of male genitalia. Another

possible explanation is that some KCS patients would not be diagnosed as KCS. Recently, Guo et al. identified a KCS patient with a R569H mutation of *FAM111A* from 14 children with severe short stature of unknown etiology by whole–exome sequencing (66). It is of note that the patient had not been suffered from hypoparathyroidism. This report highlighted the possibility that there may be more patients with KCS in short stature children of unknown etiology. As the genetic background of KCS2 was elucidated in this study, there might be the possibility that more patients with KCS would be reported.

Effective treatment for short stature in patients with bone disease is scarce, although our understanding of molecular mechanism for bone growth has been gradually growing. This is partly because of a lack of efficient method for screening and testing potential drugs (67). Recently, Yamashita et al. reported that statin treatment improved FGFR3 skeletal dysplasia dwarfism by developing a human-disease based system for screening potential drugs (68). They established a cell-based model of impaired bone growth by using induced pluripotent stem (iPS) cells. Considering recent dramatic advances in the technology of iPS cells, this method would allow us to screen potential drugs for treating short stature of another bone disease like KCS. In addition, it is notable that short stature in patients with KCS is proportionate, which implied that the

cell-based model of KCS might be very promising for exploring drugs effective for not only tubular bones but also other bones. I believe that in the long run, my finding would be contributing to discovering new drugs for short stature.

TBCE mutation causes both KCS1 and SSS, and *FAM111A* mutation causes both KCS2 and gracile bone dysplasia (8, 25, 51, 69). Clinical features of these syndromes and its causative genes were summarized in Figure 17. As these syndromes share characteristic three features (growth retardation, hypoparathyroidism, and skeletal defects) and causative genes had been identified (Figure 17), I propose that these syndromes should be designated as Kenny–Caffey related syndromes. However, some patients with these syndromes do not have a mutation in these responsible genes. This fact suggested that there may be other syndrome which could be included in this entity, and there may be other gene which would be responsible for this entity. Genetic analyses of additional patients in this entity and further investigation for exploring other responsible gene should be needed to elucidate the whole picture of this entity.

As the function of FAM111A remains largely unknown at present, I would like to clarify its function in several methods. First, I will study the molecular mechanism of cartilage proliferation and differentiation by using some cell lines like ATDC5. With these studies, I would be able to find the putative network related to *FAM111A*. Second,

I will make transgenic mice for the recurrent mutation of *FAM111A* and study expressions of FAM111A and its putative related genes in several tissues. If I could make transgenic mice that had phenotypes of KCS2, I might be able to elucidate many unidentified function of FAM111A by investigating tissues of the mice. Third, I will develop the above mentioned cell-based model of KCS by using iPS cells. With this method, I might discover new drugs for improving phenotypes of KCS2. Through these *in vitro* and *vivo* studies, I would like to elucidate the function of FAM111A one by one in the near future.

In conclusion, my finding that all four Japanese KCS2 patients analyzed in this study have the same *de novo* mutation (R569H) of *FAM111A* indicates that KCS2 is caused by a heterozygous mutation of *FAM111A*, and R569H is the hot spot mutation in patients with KCS2. Although the function of FAM111A is largely unknown, this study provides evidence that FAM111A is a key molecule for normal bone development, height gain, and PTH development and/or regulation. My finding further creates a new research area in the fields associated with shared phenotypic features in KCS and different phenotypes between KCS1 and KCS2.

[Acknowledgement]

I am grateful to Professor Akira Oka (Department of Pediatrics, Graduate School of Medicine, The University of Tokyo) for giving supervision for writing this thesis. I am also thankful to Associate Professor Sachiko Kitanaka (Department of Pediatrics, Graduate School of Medicine, The University of Tokyo) for providing the intellectual input to this thesis.

I would like to express great thanks to Professor Shoji Tsuji (Department of Neurology, Graduate School of Medicine, The University of Tokyo), Professor Shinichi Morishita (Department of Computational Biology, Graduate School of Frontier Sciences, The University of Tokyo), and Drs Koichiro Doi (Department of Computational Biology, Graduate School of Frontier Sciences, The University of Tokyo), Jun Mitsui (Department of Neurology, Graduate School of Medicine, The University of Tokyo), Hiroyuki Ishiura (Department of Neurology, Graduate School of Medicine, The University of Tokyo), Jun Yoshimura (Department of Computational Biology, Graduate School of Frontier Sciences, The University of Tokyo) for collaborating the study. I would also like to express great thanks to Drs Yoichiro Oda (Department of Pediatrics, Ohta NIshinouchi Hospital), Etsuro Tokuhiro (Department of Pediatrics,

Odawara City Hospital), Akihiro Yasoda (Department of Medicine and Clinical Science, Kyoto University Graduate School of Medicine), Tohru Yorifuji (Department of Pediatric Endocrinology and Metabolism, Children's Medical Center, Osaka City General Hospital), and Reiko Horikawa (Division of Endocrinology and Metabolism, National Center for Child Health and Development) for providing the data of patients with KCS2. And I thank patients and their family members who participated in this study.

Finally, I also would like to express thank Minako Takaki and Reiko Onai for technical supports.

This study was supported by Grant-in-Aid from the Ministry of Education, Science, Sports, and Culture of Japan.

[References]

1. Kenny FM, Linarelli L. Dwarfism and cortical thickening of tubular bones. Transient hypocalcemia in a mother and son. Am J Dis Child 111:201-207, 1966

2. Caffey J. Congenital stenosis of medullary spaces in tubular bones and calvaria in two proportionate dwarfs-mother and son; coupled with transitory hypocalcemic tetany. Am J Roentgenol Radium Ther Nucl Med 100:1-11, 1967

3. Fanconi S, Fischer JA, Wieland P, Atares M, Fanconi A, Giedion A, Prader A. Kenny syndrome: evidence for idiopathic hypoparathyroidism in two patients and for abnormal parathyroid hormone in one. J Pediatr 109:469-475,1986

4. Lee WK, Vargas A, Barnes J, Root AW. The Kenny-Caffey syndrome: growth retardation and hypocalcemia in a young boy. Am J Med Genet 14:773-782, 1983

5. Larsen JL, Kivlin J, Odell WD. Unusual cause of short stature. Am J Med 78:1025-1032, 1985

6. Majewski F, Rosendahl W, Ranke M, Nolte K. The Kenny syndrome, a rare type of growth deficiency with tubular stenosis, transient hypoparathyroidism and anomalies of refraction. Eur J Pediatr 136:21-30, 1981

7. Franceschini P, Testa A, Bogetti G, Girardo E, Guala A, Lopez-Bell G, Buzio G, Ferrario E, Piccato E. Kenny-Caffey syndrome in two sibs born to consanguineous

parents: evidence for an autosomal recessive variant. Am J Med Genet 42:112-116, 1992

8. Isojima T, Kitanaka S. Kenny-Caffey syndrome and its related syndromes (in Japanese). Nihon Rinsho 73:1959-1964, 2015

9. Moussaid Y, Griffiths D, Richard B, Dieux A, Lemerrer M, Léger J, Lacombe D, Bailleul-Forestier I. Oral manifestations of patients with Kenny-Caffey Syndrome. Eur J Med Genet 55:441-445, 2012

10. Courtens W, Wuyts W, Poot M, Szuhai K, Wauters J, Reyniers E, Eleveld M, Diaz G, Nöthen MM, Parvari R. Hypoparathyroidism-retardation-dysmorphism syndrome in a girl: A new variant not caused by a TBCE mutation-clinical report and review. Am J Med Genet A 140:611-617, 2006

11. Hoffman WH, Kovacs K, Li S, Kulharya AS, Johnson BL, Eidson MS, Cleveland WW. Kenny-Caffey syndrome and microorchidism. Am J Med Genet 80:107-111, 1998

12. Abdel-Al YK, Auger LT, el-Gharbawy F. Kenny-Caffey syndrome. Case report and literature review. Clin Pediatr (Phila) 28:175-179, 1989

13. Bergada I, Schiffrin A, Abu Srair H, Kaplan P, Dornan J, Goltzman D, Hendy GN. Kenny syndrome: description of additional abnormalities and molecular studies.

Hum Genet 80:39-42, 1988

14. Demir T, Kecik D, Cehreli ZC. Kenny-Caffey Syndrome: oral findings and 4-year follow-up of overlay denture therapy. J Dent Child (Chic) 74:236-240, 2007

15. Sabry MA, Zaki M, Shaltout A. Genotypic/phenotypic heterogeneity of Kenny-Caffey syndrome. J Med Genet 35:1054-1055, 1998

16. Sabry MA, Farag TI, Shaltout AA, Zaki M, Al-Mazidi Z, Abulhassan SJ, Al-Torki N, Quishawi A, Al Awadi SA. Kenny-Caffey syndrome: an Arab variant? Clin Genet 55:44-49, 1999

17. Wilson MG, Maronde RF, Mikity VG, Shinno NW. Dwarfism and congenital medullary stenosis (Kenny syndrome). Birth Defects Orig Artic Ser 10:128-132, 1974

18. Tahseen K, Khan S, Uma R, Usha R, Al Ghanem MM, Al Awadi SA, Farag TI. Kenny-Caffey syndrome in six Bedouin sibships: autosomal recessive inheritance is confirmed. Am J Med Genet 69:126-132, 1997

19. Sabry MA, Zaki M, Abul Hassan SJ, Ramadan DG, Abdel Rasool MA, al Awadi SA, al Saleh Q. Kenny-Caffey syndrome is part of the CATCH 22 haploinsufficiency cluster. J Med Genet 35:31-36, 1998

20. Sanjad SA, Sakati NA, Abu-Osba YK, Kaddoura R, Milner RD. A new syndrome of congenital hypoparathyroidism, severe growth failure, and dysmorphic

features. Arch Dis Child 66:193-196, 1991

21. Richardson RJ, Kirk JM. Short stature, mental retardation, and hypoparathyroidism: a new syndrome. Arch Dis Child 65:1113-1117, 1990

22. Parvari R, Hershkovitz E, Kanis A, Gorodischer R, Shalitin S, Sheffield VC, Carmi R. Homozygosity and linkage-disequilibrium mapping of the syndrome of congenital hypoparathyroidism, growth and mental retardation, and dysmorphism to a 1-cM interval on chromosome 1q42-43. Am J Hum Genet 63:163-169, 1998

23. Diaz GA, Khan KT, Gelb BD. The autosomal recessive Kenny-Caffey syndrome locus maps to chromosome 1q42-q43. Genomics 54:13-18, 1998

24. Diaz GA, Gelb BD, Ali F, Sakati N, Sanjad S, Meyer BF, Kambouris M. Sanjad-Sakati and autosomal recessive Kenny-Caffey syndromes are allelic: evidence for an ancestral founder mutation and locus refinement. Am J Med Genet 85:48-52, 1999

25. Parvari R, Hershkovitz E, Grossman N, Gorodischer R, Loeys B, Zecic A, Mortier G, Gregory S, Sharony R, Kambouris M, Sakati N, Meyer BF, Al Aqeel AI, Al Humaidan AK, Al Zanhrani F, Al Swaid A, Al Othman J, Diaz GA, Weiner R, Khan KT, Gordon R, Gelb BD, Consortium HARK-CS. Mutation of TBCE causes hypoparathyroidism-retardation-dysmorphism and autosomal recessive Kenny-Caffey

syndrome. Nat Genet 32:448-452, 2002

26. Collins FS. Positional cloning moves from perditional to traditional. Nat Genet 9:347-350, 1995

27. Biesecker LG. Exome sequencing makes medical genomics a reality. Nat Genet 42:13-14, 2010

28. Metzker ML. Sequencing technologies - the next generation. Nat Rev Genet 11:31-46, 2010

29. Shendure J, Ji H. Next-generation DNA sequencing. Nat Biotechnol 26:1135-1145, 2008

30. Bamshad MJ, Ng SB, Bigham AW, Tabor HK, Emond MJ, Nickerson DA, Shendure J. Exome sequencing as a tool for Mendelian disease gene discovery. Nat Rev Genet 12:745-755, 2011

31. Turner EH, Lee C, Ng SB, Nickerson DA, Shendure J. Massively parallel exon capture and library-free resequencing across 16 genomes. Nat Methods 6:315-316, 2009

32. Okou DT, Steinberg KM, Middle C, Cutler DJ, Albert TJ, Zwick ME. Microarray-based genomic selection for high-throughput resequencing. Nat Methods 4:907-909, 2007

33. Porreca GJ, Zhang K, Li JB, Xie B, Austin D, Vassallo SL, LeProust EM, Peck BJ, Emig CJ, Dahl F, Gao Y, Church GM, Shendure J. Multiplex amplification of large sets of human exons. Nat Methods 4:931-936, 2007

34. Mamanova L, Coffey AJ, Scott CE, Kozarewa I, Turner EH, Kumar A, Howard E, Shendure J, Turner DJ. Target-enrichment strategies for next-generation sequencing. Nat Methods 7:111-118, 2010

35. Stenson PD, Ball EV, Howells K, Phillips AD, Mort M, Cooper DN. The Human Gene Mutation Database: providing a comprehensive central mutation database for molecular diagnostics and personalized genomics. Hum Genomics 4:69-72, 2009

36. Ng SB, Turner EH, Robertson PD, Flygare SD, Bigham AW, Lee C, Shaffer T, Wong M, Bhattacharjee A, Eichler EE, Bamshad M, Nickerson DA, Shendure J. Targeted capture and massively parallel sequencing of 12 human exomes. Nature 461:272-276, 2009

37. Rabbani B, Mahdieh N, Hosomichi K, Nakaoka H, Inoue I. Next-generation sequencing: impact of exome sequencing in characterizing Mendelian disorders. J Hum Genet 57:621-632, 2012

38. Ku CS, Naidoo N, Pawitan Y. Revisiting Mendelian disorders through exome sequencing. Hum Genet 129:351-370, 2011

39. Ng SB, Buckingham KJ, Lee C, Bigham AW, Tabor HK, Dent KM, Huff CD, Shannon PT, Jabs EW, Nickerson DA, Shendure J, Bamshad MJ. Exome sequencing identifies the cause of a mendelian disorder. Nat Genet 42:30-35, 2010

40. Ng SB, Bigham AW, Buckingham KJ, Hannibal MC, McMillin MJ, Gildersleeve HI, Beck AE, Tabor HK, Cooper GM, Mefford HC, Lee C, Turner EH, Smith JD, Rieder MJ, Yoshiura K, Matsumoto N, Ohta T, Niikawa N, Nickerson DA, Bamshad MJ, Shendure J. Exome sequencing identifies MLL2 mutations as a cause of Kabuki syndrome. Nat Genet 42:790-793, 2010

41. Hoischen A, van Bon BW, Gilissen C, Arts P, van Lier B, Steehouwer M, de Vries P, de Reuver R, Wieskamp N, Mortier G, Devriendt K, Amorim MZ, Revencu N, Kidd A, Barbosa M, Turner A, Smith J, Oley C, Henderson A, Hayes IM, Thompson EM, Brunner HG, de Vries BB, Veltman JA. De novo mutations of SETBP1 cause Schinzel-Giedion syndrome. Nat Genet 42:483-485, 2010

42. Wang JL, Yang X, Xia K, Hu ZM, Weng L, Jin X, Jiang H, Zhang P, Shen L, Guo JF, Li N, Li YR, Lei LF, Zhou J, Du J, Zhou YF, Pan Q, Wang J, Li RQ, Tang BS. TGM6 identified as a novel causative gene of spinocerebellar ataxias using exome sequencing. Brain 133:3510-3518, 2010

43. Sirmaci A, Walsh T, Akay H, Spiliopoulos M, Sakalar YB,

Hasanefendioğlu-Bayrak A, Duman D, Farooq A, King MC, Tekin M. MASP1 mutations in patients with facial, umbilical, coccygeal, and auditory findings of Carnevale, Malpuech, OSA, and Michels syndromes. Am J Hum Genet 87:679-686, 2010

44. Pierce SB, Walsh T, Chisholm KM, Lee MK, Thornton AM, Fiumara A, Opitz JM, Levy-Lahad E, Klevit RE, King MC. Mutations in the DBP-deficiency protein HSD17B4 cause ovarian dysgenesis, hearing loss, and ataxia of Perrault Syndrome. Am J Hum Genet 87:282-288, 2010

45. Vissers LE, de Ligt J, Gilissen C, Janssen I, Steehouwer M, de Vries P, van Lier B, Arts P, Wieskamp N, del Rosario M, van Bon BW, Hoischen A, de Vries BB, Brunner HG, Veltman JA. A de novo paradigm for mental retardation. Nat Genet 42:1109-1112, 2010

46. Girard SL, Gauthier J, Noreau A, Xiong L, Zhou S, Jouan L, Dionne-Laporte A, Spiegelman D, Henrion E, Diallo O, Thibodeau P, Bachand I, Bao JY, Tong AH, Lin CH, Millet B, Jaafari N, Joober R, Dion PA, Lok S, Krebs MO, Rouleau GA. Increased exonic de novo mutation rate in individuals with schizophrenia. Nat Genet 43:860-863, 2011

47. Tadaki H, Tokuhiro E, Shiga K, Kikuchi N, Mukai N, Fujieda K. A Case of a

2-Year-Old Girl with Kenny-Caffey Syndrome Type2. Clinical Pediatric Endocrinology 14:22 (Abstract from the 39th annual scientific meeting of the Japanese society for pediatric endocrinology), 2005

48. Oda Y, Ono R, Hiwatari M, Iwasaki H, Namai Y, Iimori Y. A Case Report: Three-Year-Old Boy of Kenny-Caffey Syndrome Type 2. Clinical Pediatric Endocrinology 9:140 (Abstract from the 34th annual scientific meeting of the Japanese society for pediatric endocrinology), 2000

49. Yorifuji T, Muroi J, Uematsu A. Kenny-Caffey syndrome without the CATCH 22 deletion. J Med Genet 35:1054, 1998

50. Izumi Y, Tanae A, Kuratsuji T, Kindaichi J, Ohshima T, Nihei K, Fujimoto J, Hibi I, Kohsaka T, Hori M, Kobayashi N. A case of 12-year-old boy with Kenny syndrome associated with hypomagnesemia and humoral immunodeficiency (in Japanese). Shoninaika 19:1503-1512, 1987

51. Unger S, Górna MW, Le Béchec A, Do Vale-Pereira S, Bedeschi MF, Geiberger S, Grigelioniene G, Horemuzova E, Lalatta F, Lausch E, Magnani C, Nampoothiri S, Nishimura G, Petrella D, Rojas-Ringeling F, Utsunomiya A, Zabel B, Pradervand S, Harshman K, Campos-Xavier B, Bonafé L, Superti-Furga G, Stevenson B, Superti-Furga A. FAM111A Mutations Result in Hypoparathyroidism and Impaired

Skeletal Development. Am J Hum Genet 92: 990-995, 2013

52. Li H, Durbin R. Fast and accurate short read alignment with Burrows-Wheeler transform. Bioinformatics 25:1754-1760, 2009

53. Li H, Handsaker B, Wysoker A, Fennell T, Ruan J, Homer N, Marth G, Abecasis G, Durbin R, Subgroup GPDP. The Sequence Alignment/Map format and SAMtools. Bioinformatics 25:2078-2079, 2009

54. Kong A, Frigge ML, Masson G, Besenbacher S, Sulem P, Magnusson G, Gudjonsson SA, Sigurdsson A, Jonasdottir A, Wong WS, Sigurdsson G, Walters GB, Steinberg S, Helgason H, Thorleifsson G, Gudbjartsson DF, Helgason A, Magnusson OT, Thorsteinsdottir U, Stefansson K. Rate of de novo mutations and the importance of father's age to disease risk. Nature 488:471-475, 2012

55. Fine DA, Rozenblatt-Rosen O, Padi M, Korkhin A, James RL, Adelmant G, Yoon R, Guo L, Berrios C, Zhang Y, Calderwood MA, Velmurgan S, Cheng J, Marto JA, Hill DE, Cusick ME, Vidal M, Florens L, Washburn MP, Litovchick L, DeCaprio JA. Identification of FAM111A as an SV40 host range restriction and adenovirus helper factor. PLoS Pathog 8:e1002949, 2012

56. Akamatsu S, Takata R, Haiman CA, Takahashi A, Inoue T, Kubo M, Furihata M, Kamatani N, Inazawa J, Chen GK, Le Marchand L, Kolonel LN, Katoh T, Yamano Y,

Yamakado M, Takahashi H, Yamada H, Egawa S, Fujioka T, Henderson BE, Habuchi T, Ogawa O, Nakamura Y, Nakagawa H. Common variants at 11q12, 10q26 and 3p11.2 are associated with prostate cancer susceptibility in Japanese. Nat Genet 44:426-429, S421, 2012

57. Shiang R, Thompson LM, Zhu YZ, Church DM, Fielder TJ, Bocian M, Winokur ST, Wasmuth JJ. Mutations in the transmembrane domain of FGFR3 cause the most common genetic form of dwarfism, achondroplasia. Cell 78:335-342, 1994

58. Weinstein LS, Shenker A, Gejman PV, Merino MJ, Friedman E, Spiegel AM. Activating mutations of the stimulatory G protein in the McCune-Albright syndrome. N Engl J Med 325:1688-1695, 1991

59. Gensure RC, Mäkitie O, Barclay C, Chan C, Depalma SR, Bastepe M, Abuzahra H, Couper R, Mundlos S, Sillence D, Ala Kokko L, Seidman JG, Cole WG, Jüppner H. A novel COL1A1 mutation in infantile cortical hyperostosis (Caffey disease) expands the spectrum of collagen-related disorders. J Clin Invest 115:1250-1257, 2005

60. Shoback D. Clinical practice. Hypoparathyroidism. N Engl J Med 359:391-403, 2008

61. Zajac JD, Danks JA. The development of the parathyroid gland: from fish to human. Curr Opin Nephrol Hypertens 17:353-356, 2008

62. Boynton JR, Pheasant TR, Johnson BL, Levin DB, Streeten BW. Ocular findings in Kenny's syndrome. Arch Ophthalmol 97:896-900, 1979

63. Parvari R, Diaz GA, Hershkovitz E. Parathyroid development and the role of tubulin chaperone E. Horm Res 67:12-21, 2007

64. Horton WA, Hall JG, Hecht JT. Achondroplasia. Lancet 370:162-172, 2007

65. Nikkel SM, Ahmed A, Smith A, Marcadier J, Bulman DE, Boycott KM. Mother-to-daughter transmission of Kenny-Caffey syndrome associated with the recurrent, dominant FAM111A mutation p.Arg569His. Clin Genet 86:394-395, 2014

66. Guo MH, Shen Y, Walvoord EC, Miller TC, Moon JE, Hirschhorn JN, Dauber A. Whole exome sequencing to identify genetic causes of short stature. Horm Res Paediatr 82:44-52, 2014

67. Olsen BR. Disease models: Statins give bone growth a boost. Nature 513:494-495, 2014

68. Yamashita A, Morioka M, Kishi H, Kimura T, Yahara Y, Okada M, Fujita K, Sawai H, Ikegawa S, Tsumaki N. Statin treatment rescues FGFR3 skeletal dysplasia phenotypes. Nature 513:507-511, 2014

69. Isojima T, Doi K, Mitsui J, Oda Y, Tokuhiro E, Yasoda A, Yorifuji T, Horikawa R, Yoshimura J, Ishiura H, Morishita S, Tsuji S, Kitanaka S. A recurrent de

novo FAM111A mutation causes Kenny-Caffey syndrome type 2. J Bone Miner Res 29:992-998, 2014

[Tables]

Table 1: Clinical characteristics of four unrelated Japanese patients with sporadic Kenny-Caffey syndrome type 2 (KCS2)

Patient number	I-1	II-4	III-9	IV-13
Gender	Female	Male	Female	Male
Birth weight	3,094 g (0.3 SD)	2,882 g (-0.4 SD)	2,750 g (-0.5 SD)	2,900 g (-0.3 SD)
Birth length	47.5 cm (-0.4 SD)	50.0 cm (0.5SD)	46 cm (-1.1 SD)	46 cm (-1.4 SD)
Hypoparathyroidism	Yes	Yes	Yes	Yes
Hypomagnesemia	Yes	Yes	Yes	Yes
Short stature	Yes	Yes	Yes	Yes
Mental retardation	No	No	No	No
Tubular bone finding[1)]	Yes	Yes	Yes	Yes
Anterior fontanelle[2)]	Yes	Yes	Yes	Yes
Eye abnormalities	Hypermetropia, Pseudopapilledema	Hypermetropia	Hypermetropia	Hypermetropia , Amblyopia, Pseudopapilledema
GHD[3)]	Severe GHD	Mild GHD	No	No
Age at diagnosis	2 years	4 years	5 years	12 years
Age at follow-up	10 years	16 years	22 years	38 years
Height at last follow-up	110.8 cm (-4.2SD)	120.6 cm (-8.2 SD)	134 cm (-4.5 SD)	140cm (-5.3 SD)
Other features	Infantile liver dysfunction, Polysyndactyly, anemia	Severe atopic dermatitis	Hypothalamic amenorrhea	Humoral immunodeficiency

[1)] Cortical thickening and medullary stenosis of the tubular bones,[2)] Delayed closure of anterior fontanelle, [3)] Growth hormone deficiency

Table 2: Statistics of exome sequencing experiments in this study

Sample number	Reads	Mapped reads	Mapping Rate (%)	Target coverage >10x	Coverage(x)
I-1	100,588,416	98,978,316	98.40	92.01	147.66
I-2	120,057,198	118,622,122	98.80	93.51	177.03
I-3	123,580,080	122,049,696	98.76	93.52	182.15
II-4	102,877,966	101,492,454	98.65	92.63	151.41
II-5	78,363,868	77,202,661	98.52	91.36	115.69
II-6	88,778,654	87,327,784	98.37	92.07	130.88
III-9	92,622,462	91,125,885	98.38	91.92	136.89
III-10	80,820,926	79,540,594	98.42	90.88	119.42
III-11	69,884,892	68,675,010	98.27	89.60	103.15

Table 3: Primers and PCR conditions used to amplify the coding region of *TBCE*

Primer name	Sequence 5'-3'	Product size	Annealing temperature
TBCEe1F	GTCATCCCAGGTTTCAGCAC	361 bp	60 °C
TBCEe1R	GGCTCTGGCAATCTGGGAAG		
TBCEe2F	TTCTTATCAGTGTTGTATTTTTCTTCC	285 bp	60 °C
TBCEe2R	GCTTACACAGAAACAGCTGCAA		
TBCEe3F	ACTTGTCCATTCCCTCCTCC	302 bp	60 °C
TBCEe3R	TTCTTCCTCTCCATCCCTCC		
TBCEe4F	TTTATGGCCTTTCTTGGTGG	353 bp	60 °C
TBCEe4R	ACCAGTTTAGGAGCAAAGTC		
TBCEe5F	AATTTGGGTGGTGGTTACTG	332 bp	60 °C
TBCEe5R	AAGGAAGTTGTCAAGACTGG		
TBCEe6F	GCTCATGCTCTGGAATTAAG	335 bp	60 °C
TBCEe6R	TCAGCCTGAGTAATTCCTTC		
TBCEe7F	ACCCAGATTGTTGCTTTC	402 bp	60 °C
TBCEe7R	TGAGATAGGACATGGATTTC		
TBCEe8F	TGAGGCACTTGTTTGCTG	347 bp	60 °C
TBCEe8R	TCTAATTTGTGAAGGCAATG		
TBCEe9F	AGGGACCACTCAGGTTG	357 bp	60 °C
TBCEe9R	ATTCCATCATTGTTACCACG		
TBCEe10-11F	AAGAGTTCACTTTGCATGTC	465 bp	60 °C
TBCEe10-11R	AGAAGGAACCTCCAAACTC		
TBCEe12F	GGGACATGCTTTCCTGTTG	345 bp	60 °C
TBCEe12R	AGCCTCCCAAAGTGCTG		
TBCEe13F	GCATGTGCTATGGAGGAAG	372 bp	60 °C
TBCE e13R	CAAGAAGCCCAGGAAAGG		
TBCEe14F	TCTCTGGACGCTTACCTATC	358 bp	60 °C
TBCEe14R	ATCACACCACTGCACTCC		
TBCEe15F	GGCCATCTGTTGATGTGTG	249 bp	60 °C
TBCEe15R	TCTGAGGTCCACACTTTGAG		
TBCEe16F	TGCAATGATACTGTGGTCTC	326 bp	60 °C
TBCEe16R	CCAGGCAGTAGCTTACC		
TBCEe17F	TTAAGGGTAAGCTACTGCCTG	633 bp	60 °C
TBCEe17R	CCCAAGTTTAAGGGACATTTC		

Table 4: Primers and PCR conditions used to amplify the coding region of *FAM111A*.

Primer	Sequence 5'-3'	Product size	Annealing temperature
FAM111Ae4F	AGGGAGAGCAAGGTTGGAGC	530 bp	54 ℃
FAM111Ae4R	GAGTGTGCCTGAACTAAACGTGC		
FAM111Ae5-1F	AAAGACTCGGGTTGCATTCAG	665 bp	54 ℃
FAM111Ae5-1R	AGAAATCTGCCATCCTTGCAC		
FAM111Ae5-2F	CAGGCAGGACAAAGCATCG	700 bp	50 ℃
FAM111Ae5-2R	ACCAATTATGGTTGCCCACTTAC		
FAM111Ae5-3F	TGGGTACTTATTCTGGGACAGTG	899 bp	54 ℃
FAM111Ae5-3R	GCCTGGCAGATAGGAAATGG		

Table 5: The results of filtering for detecting candidate genes for KCS2

Pedigree	Possible SNVs and indels	After filtering step 1	After filtering step 2	After filtering step 3
I	11,024	118	16	5
II	10,828	157	13	5
III	11,020	93	9	6

[Figures]

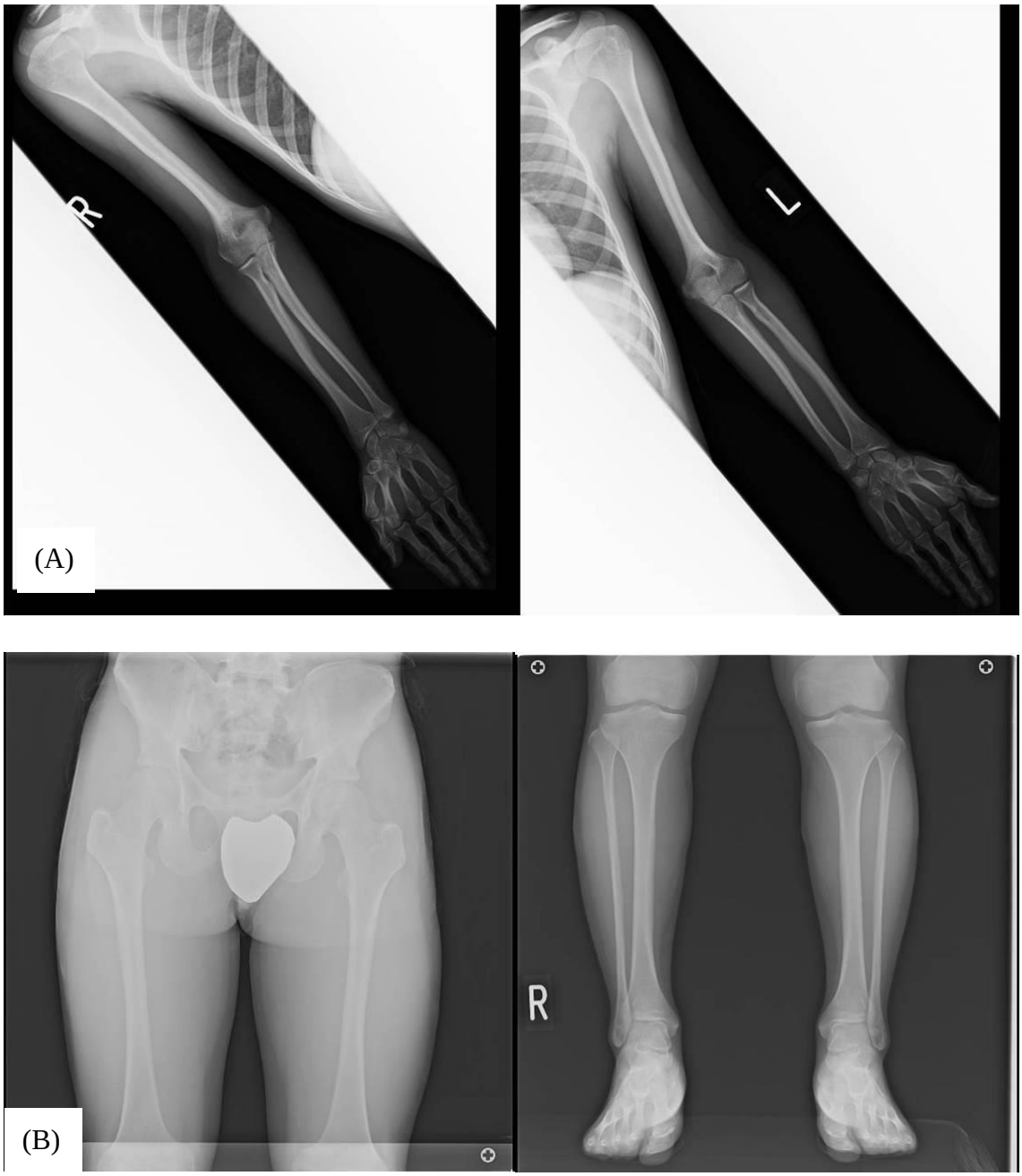

Figure 1: Radiographs of a patient with Kenny-Caffey syndrome.
(A) Upper limbs, (B) Lower limbs
Cortical thickening and medullary stenosis of tubular bones were detected.

Figure 2: Radiographs of the skull of an 18-year old patient with Kenny-Caffey syndrome.

Anterior fontanelle is open, and the calvaria is a thin sclerotic plate without a diploic space. Dental anomalies were also detected.

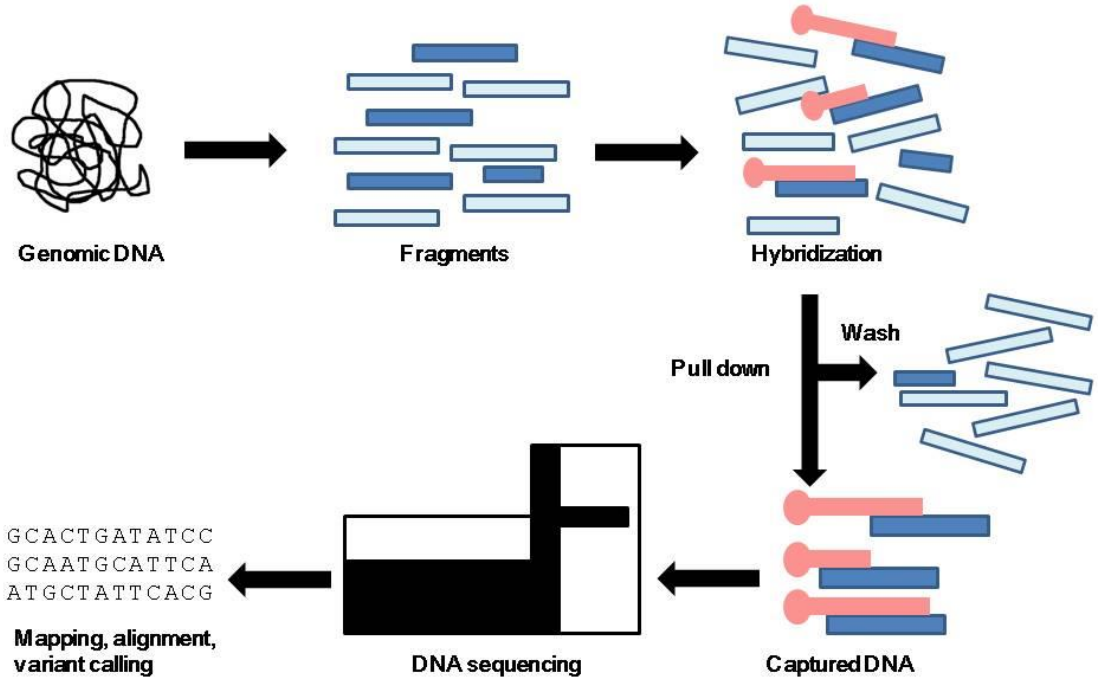

Figure 3: Conceptual diagram of an exome sequencing.

Genomic DNA is fractionated to fragment templates. (Dark blue fragments indicated exons.) These fragments are hybridized to adaptors which were designed around exons (pink fragments termed “bait”). With these fragments, biotin-streptavidin-based pulldown is performed. It is followed by amplification and massively parallel sequencing of the enriched and amplified library. Finally, the mapping and calling of candidate causal variant were explored.

This figure was drawn by referencing and modifying the review by Bamshad MJ, et al (30).

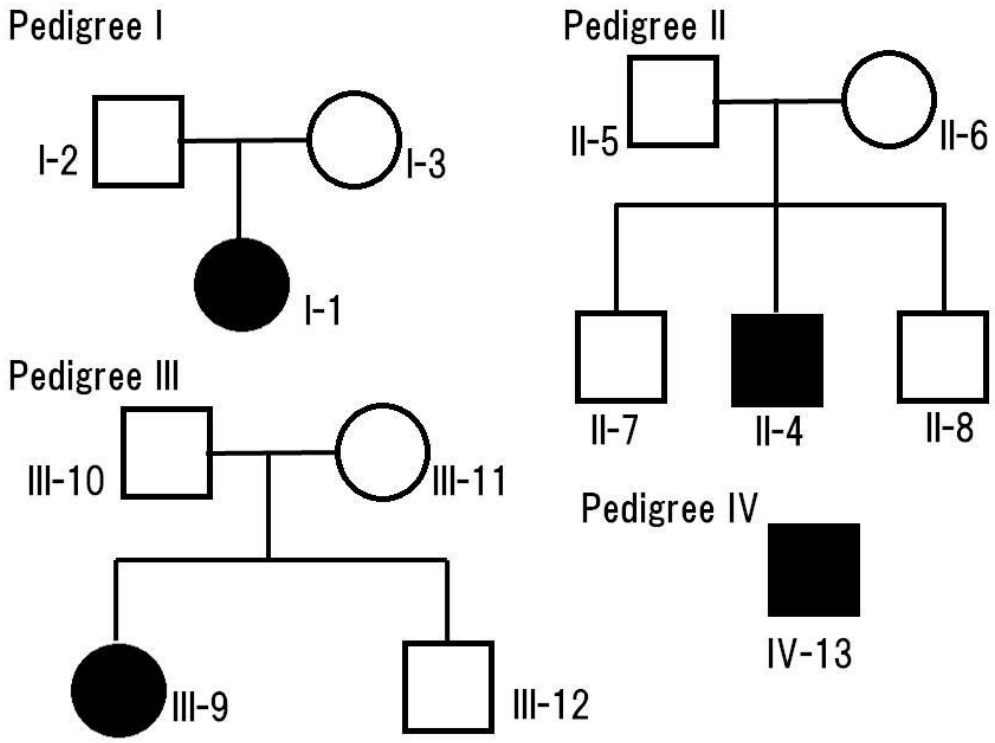

Figure 4: **Four pedigrees analyzed in this study.**
A black symbol represents the proband, a square indicates a male, and a circle shows a female.

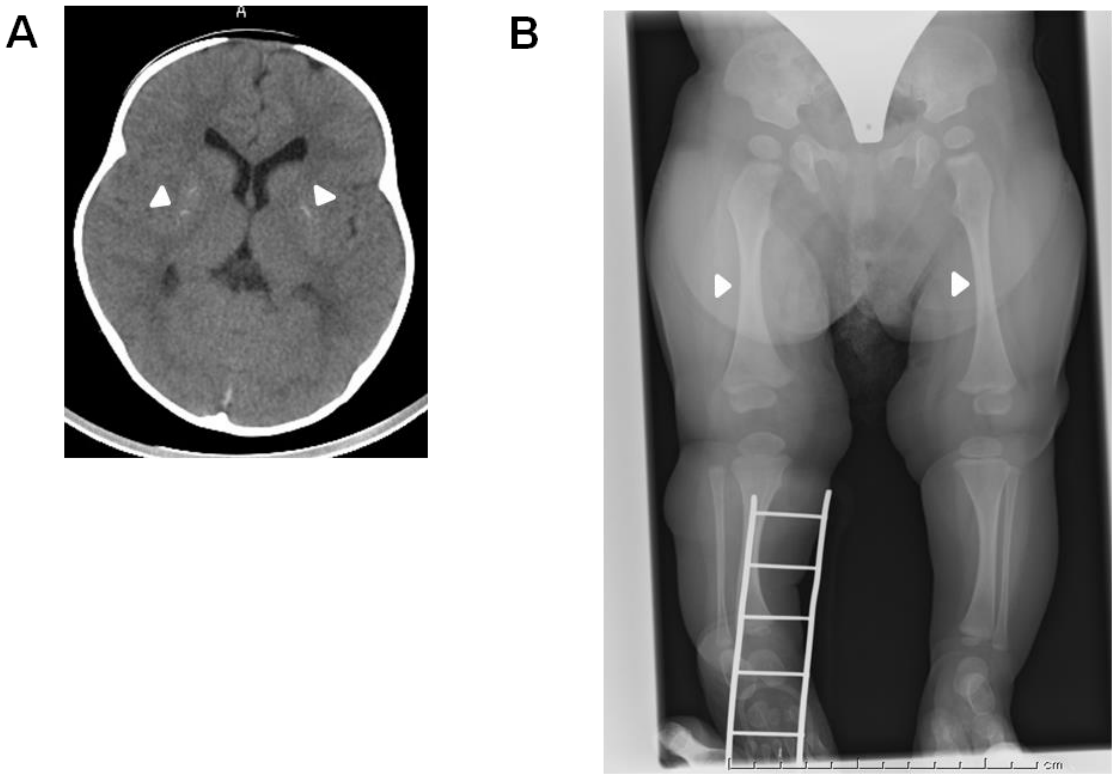

Figure 5: **Radiographic studies of case 1(proband I-1)**

A. Brain computed tomography

The arrowheads indicate calcification in the basal ganglia.

B. Radiograph at diagnosis

Cortical thickening and medullary stenosis are evident. The object shown in the right leg is used for fixing a peripheral catheter.

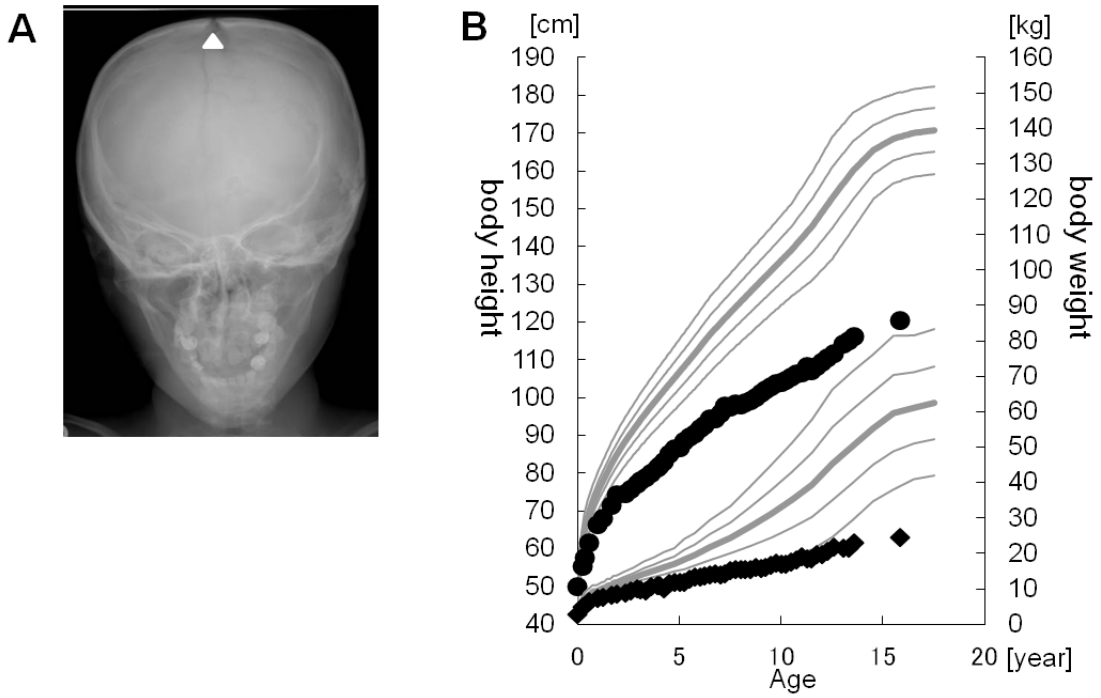

Figure 6: Radiographic study and growth chart of case 2 (proband II-4).

A. Radiograph of case 2 at nine years.

It is of note that the anterior fontanelle is open.

B. Growth chart of case 2 superimposed on the standard growth chart for a Japanese boy.

Black circles indicate the patient's height and black squares indicate his weight.

Figure 7: Radiographic study of case 3 (proband III-9).
Cortical thickening and medullary stenosis can be observed.

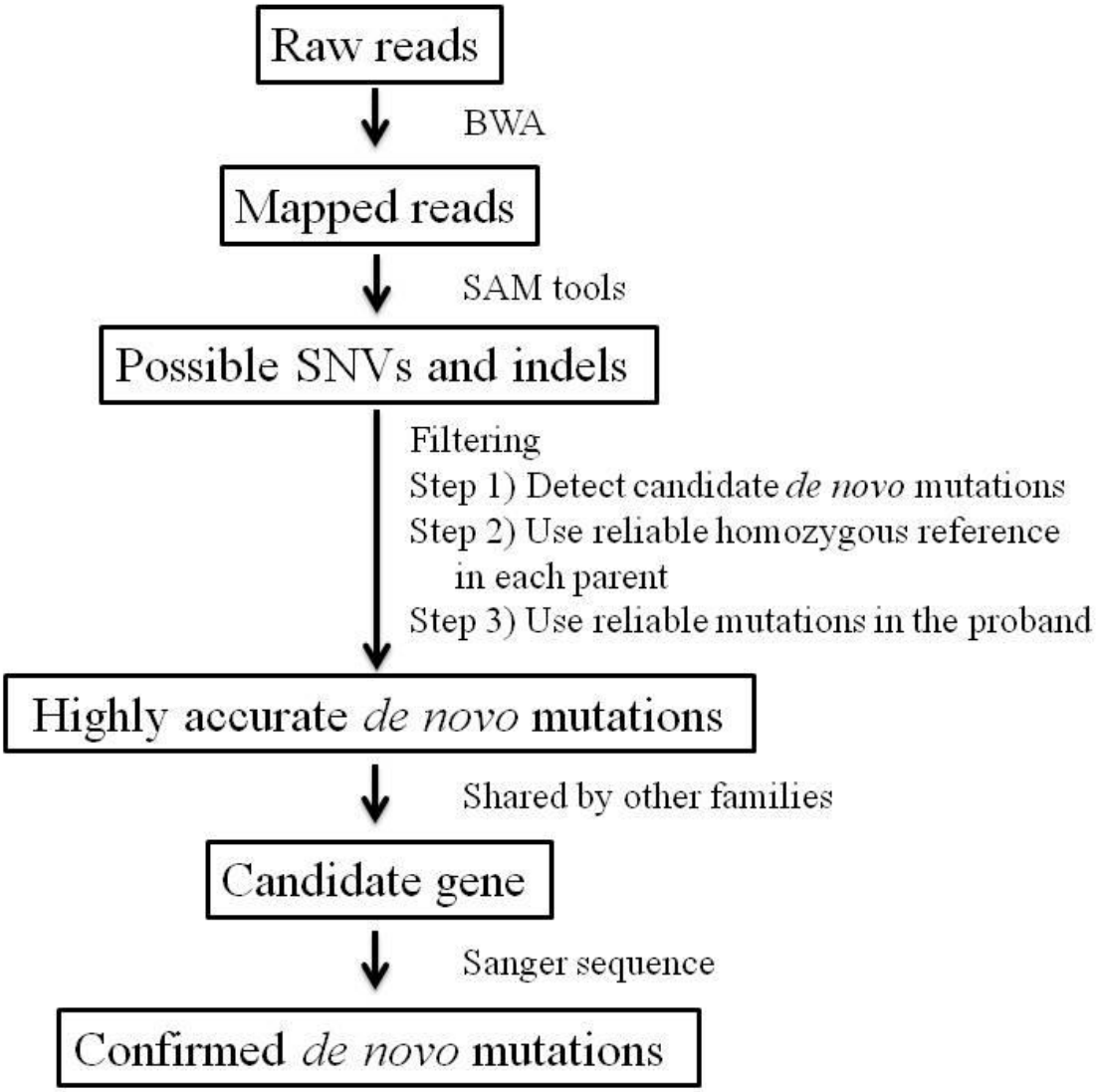

Figure 8: Pipeline for the detection of novel *de novo* mutations.

This pipeline was used to identify pathogenic mutations of Kenny–Caffey syndrome type 2. All genetic variants detected by exome sequencing were sequentially filtered through the pipeline described in the Methods section. BWA: Burrows-Wheeler Aligner

Pedigree I

chr	pos	ref	alt	dbSNP	gene
11	58920847	G	A	-	*FAM111A*
14	20181274	T	C	-	*OR11H2*
17	3807280	C	T	-	*P2RX1*
19	12542653	T	G	+	*ZNF443*
19	12542654	T	A	+	*ZNF443*

Pedigree II

chr	pos	ref	alt	dbSNP	gene
2	240981541	G	C	-	*PRR21*
2	240981583	C	A	-	*PRR21*
2	240981795	A	G	-	*PRR21*
11	58920847	G	A	-	*FAM111A*
11	72408055	G	C	+	*ARAP1*

Pedigree III

chr	pos	ref	alt	dbSNP	gene
1	230931020	C	G	-	*CAPN9*
2	219602499	G	C	+	*TTLL4*
3	124281844	C	A	+	*KALRN*
4	190904030	T	C	+	*TUBB4Q*
11	58920847	G	A	-	*FAM111A*
14	103426014	A	G	-	*CDC42BPB*

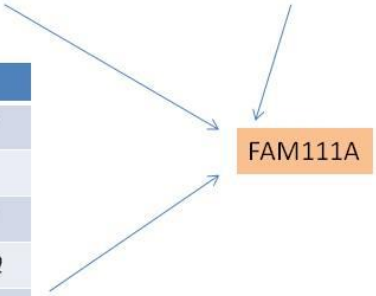

Figure 9: Candidate genes for KCS2 detected after the filtering method established in this study.

After using the three filtering steps mentioned in the text, several candidate genes were detected. Among these genes, only one single gene, *FAM111A* (NM_001142519.1), was shared among all three families. chr: chromosome number; pos: position; ref: reference nucleotide; alt: altered nucleotide; db SNP: data base single nucleotide polymorphism

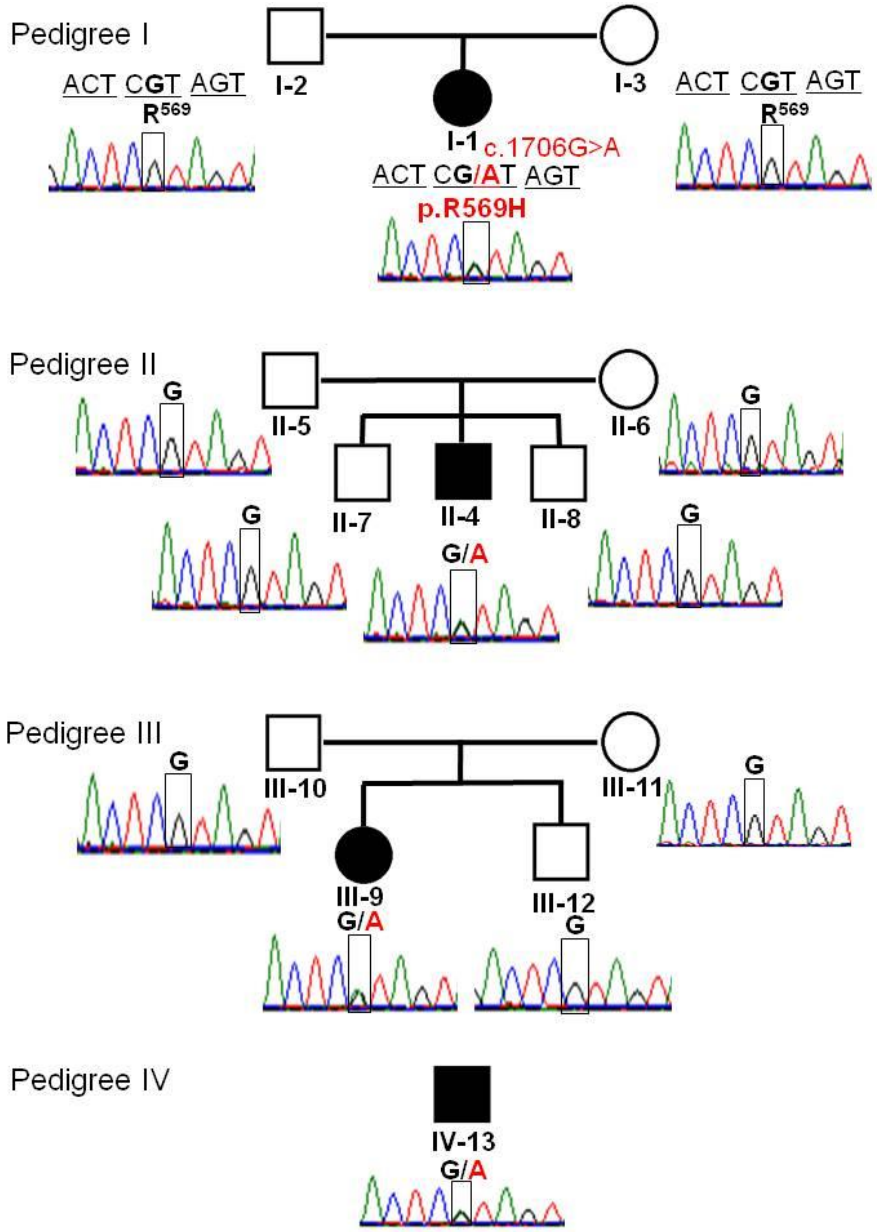

Figure 10: Four pedigrees analyzed in this study, showing the chromatograms of Sanger sequencing reactions of the *FAM111A* mutation in patients and family members.

Data were obtained by Sanger sequencing during the confirmation process. All mutations were checked by bidirectional sequencing. In each pedigree, a black symbol represents the proband, a square indicates a male, and a circle shows a female. In the chromatogram, black letters indicate the wild-type nucleotide sequence. Nucleotides in red indicate mutations. R569H was identified in all probands but not in any of the unaffected family members.

(A)

		Found in dbSNP?		PROVEAN Prediction			SIFT Prediction*		
	Total	Yes	No (novel)	Neutral	Deleterious	Not available	Tolerated	Damaging	Not available
Protein-coding	1	0	1	1	0	0	1	0	0
(1) Single AA Change	1	0	1	1	0	0	1	0	0

(B)

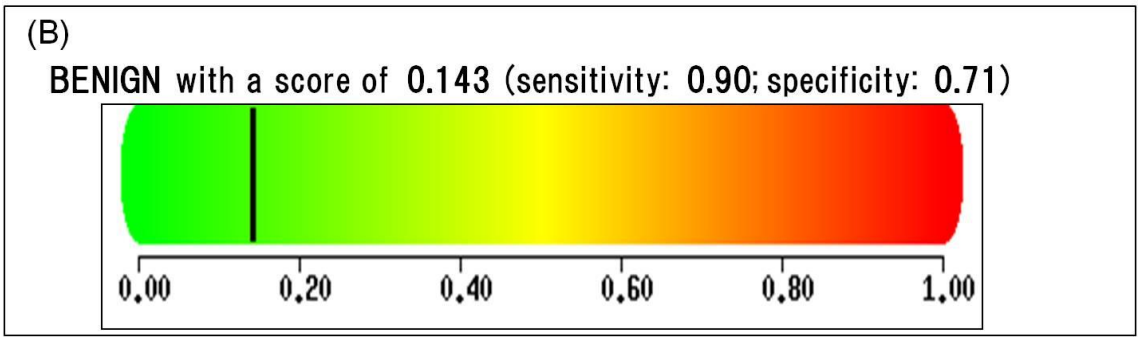

Figure 11: The result of *in silico* analyses about R569H, the hot spot *FAM111A* mutation for Kenny–Caffey syndrome type 2.

A. SIFT

SIFT analysis predicted R569H as tolerated.

B. PolyPhen2

PolyPhen2 analysis predicted R569H as benign with a score of 0.143.

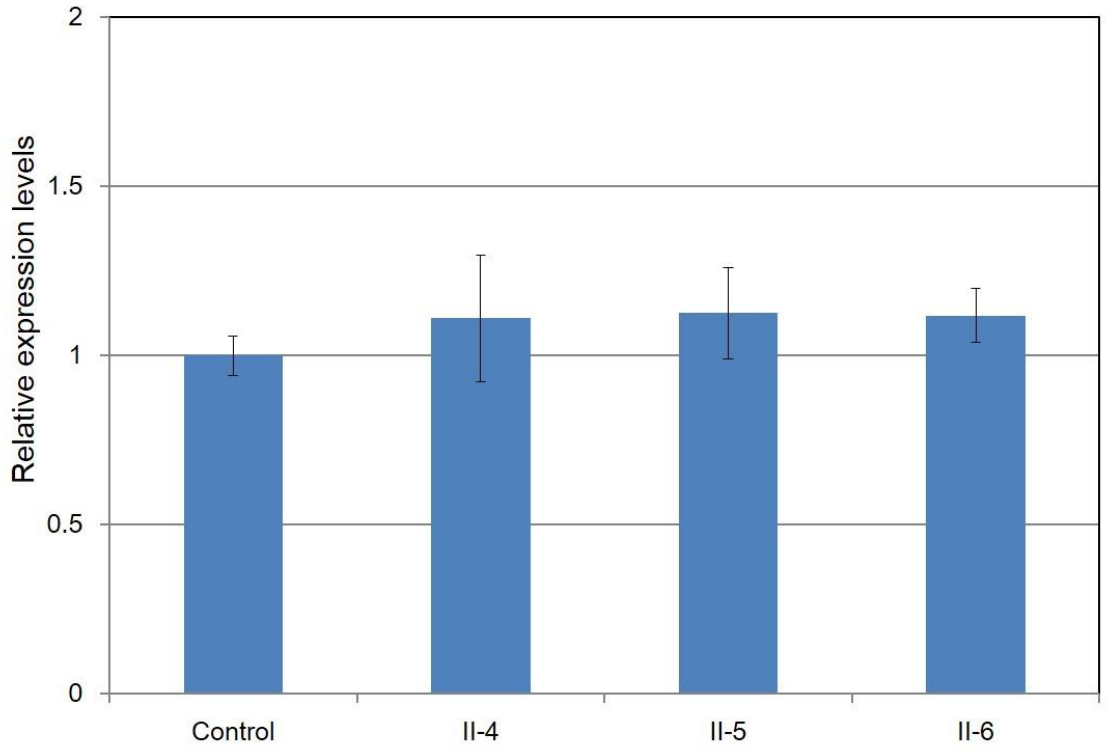

Figure 12: Relative expression levels of FAM111A.

Relative expression levels were calculated by the comparative C_T method. II-4 represent the patient with KCS2 (case2), and II-5 and II-6 are his parents. Fold changes were relative expression levels of normal control. GAPDH gene expression was used as an endogenous control. Data were expressed as mean ±SD (n= 3). *FAM111A* expression level in the patient was comparable with those in unaffected family members and normal control.

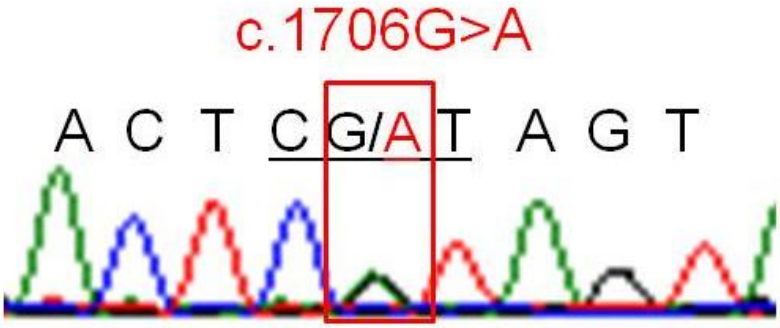

Figure 13: Direct sequencing of the RT-PCR product of II-4

Direct sequencing of the RT-PCR product of II-4 was performed by Sanger sequencing as for DNA samples. This analysis identified that the mutant and wild-type *FAM111A* were equivalently expressed in the patient.

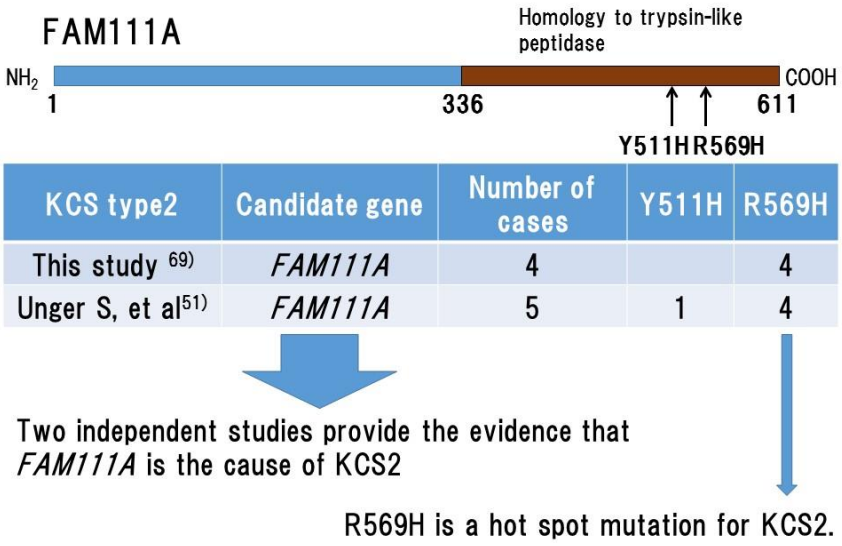

Figure 14: Mutations identified in two independent studies.

FAM111A encodes a protein consisting of 611 amino acids, and its carboxy-terminal half has homology to trypsin-like peptidases. However, the function of FAM111A is largely unknown at present.

Four of the five patients with KCS2 from different countries identified in another independent research group from Switzerland had the same R569H mutation as detected in the patients investigated in the present study. Therefore, my study together with another study from Switzerland group confirmed that FAM111A is the causative gene for KCS2, and R569H is a hot spot mutation of KCS2.

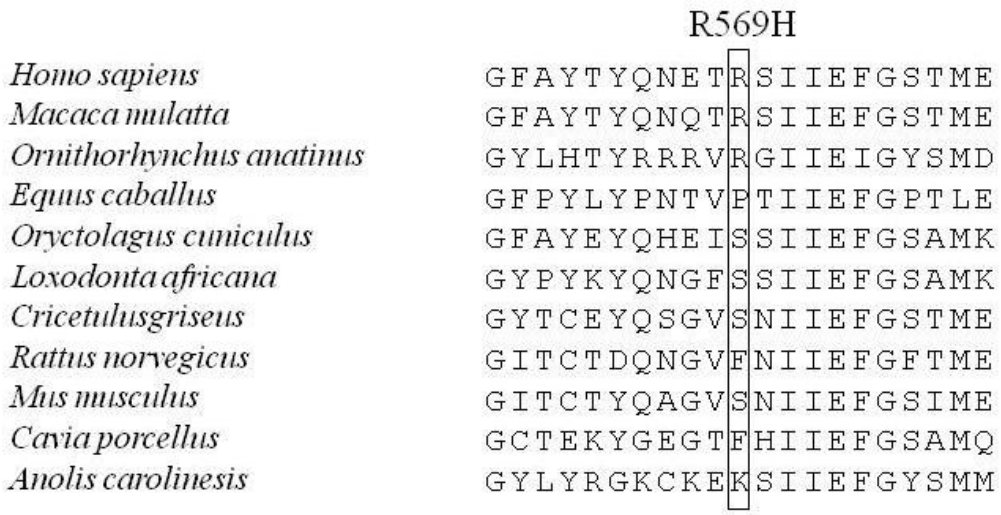

Figure 15: **Homologous comparison of the altered protein.**
Letters in the rectangular box indicate the human *FAM111A* R569 residue. It is of note that R569 is not well conserved among various species.

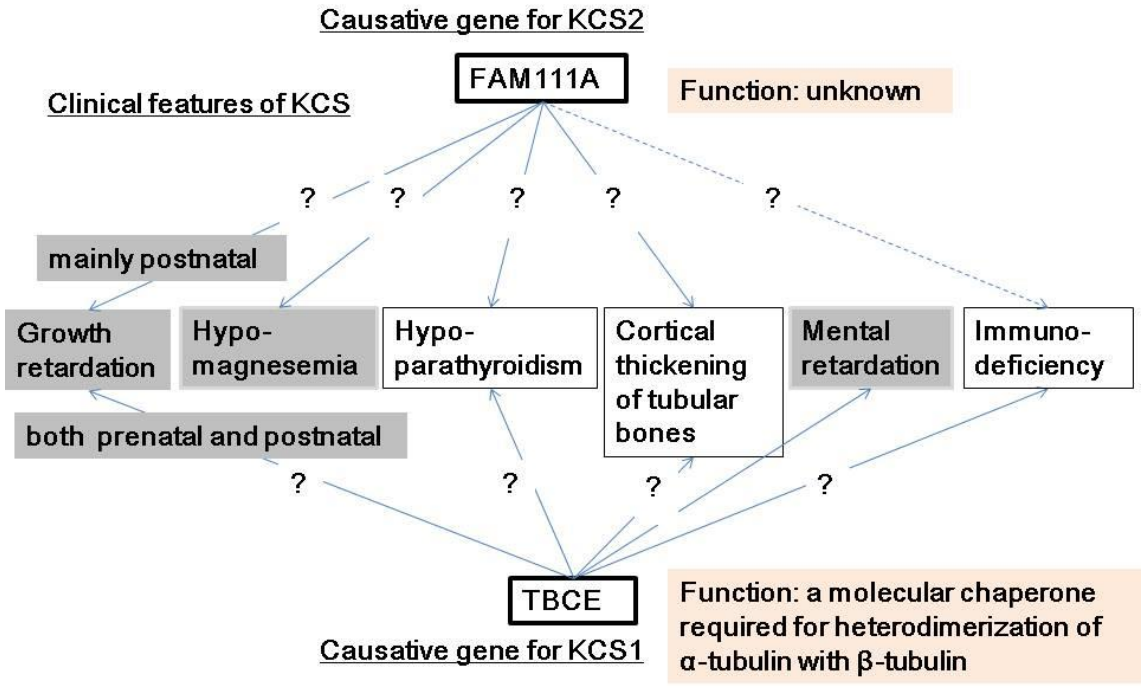

Figure 16: Shared and different phenotypic features in KCS.

Clinical features in gray-shaded rectangular boxes indicate different phenotypic features between KCS1 and KCS2. It is unknown whether immunodeficiency is a clinical feature of KCS2.

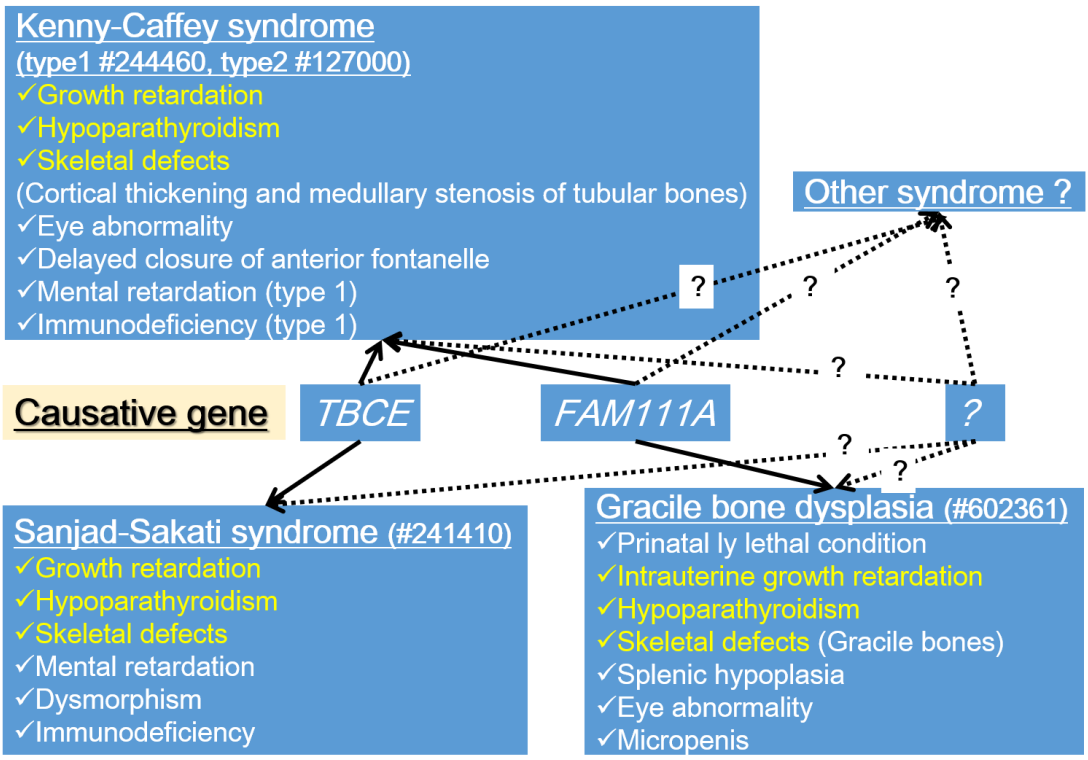

Figure 17: KCS and its related syndrome.

TBCE mutation causes both KCS1 and Sanjad-Sakati syndrome, and *FAM111A* mutation causes both KCS2 and gracile bone dysplasia. These syndromes share characteristic three features (growth retardation, hypoparathyroidism, and skeletal defects: yellow letters). These syndromes could be designated as Kenny–Caffey related syndrome. There may be other syndrome which could be included in this entity, and there may be other gene which would be responsible for this entity.

[Abbreviations]

KCS:	Kenny–Caffey syndrome
KCS1:	Kenny–Caffey syndrome type 1
KCS2:	Kenny–Caffey syndrome type 2
SSS:	Sanjad–Sakati syndrome
HRD:	Hypoparathyroidism–Retardation–Dysmorphism
STR:	Short tandem repeat marker
TBCE:	Tubulin-folding cofactor E
NGS:	Next–generation DNA sequencing
FAM111A:	Family with sequence similarity 111, member A
AST:	Aspartate aminotransferase
ALT:	Alanine aminotransferase
IGF-1:	Insulin-like growth factor 1
Ca:	Calcium
P:	Phosphorus
PTH:	Parathyroid hormone
Mg:	Magnesium
CT:	Computed tomography
GHD:	Growth hormone deficiency
BWA:	Burrows-Wheeler Aligner
SNV:	Single-nucleotide variant
PCR:	Polymerase chain reaction
RT-PCR:	Reverse-transcribed PCR
SNP:	Single-nucleotide polymorphism
SIFT:	Sorting Intolerant From Tolerant
PolyPhen:	Polymorphism Phenotyping
LT:	Large T
COL1A1:	Collagen type1 alpha 1
FGFR3:	Fibroblast growth factor receptor 3
iPS:	Induced pluripotent stem